Research Square

Preprints are preliminary reports that have not undergone peer review.
They should not be considered conclusive, used to inform clinical practice,
or referenced by the media as validated information.

Molecular and pharmacological investigation of alpha 7 nicotinic acetylcholine receptors in human induced pluripotent stem cell-derived dentate gyrus granule cells

Katalin Vincze
Semmelweis University
Edit Hathy
Semmelweis University
Krisztina Pesti
HUN-REN Institute of Agricultural Sciences
Gergő Vőfély
HUN-REN Research Centre for Natural Sciences
Eszter Szabó
HUN-REN Research Centre for Natural Sciences
Csongor Tordai
Semmelweis University
László Homolya
HUN-REN Research Centre for Natural Sciences
Zsófia Nemoda
Semmelweis University
Arpad Mike
Eötvös Loránd University
Ágota Apáti
HUN-REN Research Centre for Natural Sciences
János M Réthelyi
rethelyi.janos@semmelweis.hu

Semmelweis University

Research Article

Keywords: human iPSC, neuronal differentiation, hippocampus, dentate gyrus, granule cells, α7nAChR, pharmacological characterization

Posted Date: March 16th, 2026

DOI: https://doi.org/10.21203/rs.3.rs-9081171/v1

License: This work is licensed under a Creative Commons Attribution 4.0 International License.
Read Full License

Additional Declarations: No competing interests reported.

Data Availability Statements

The datasets generated during and/or analysed during the current study are available from the corresponding author upon reasonable request.

Molecular and pharmacological investigation of alpha 7 nicotinic acetylcholine receptors in human induced pluripotent stem cell-derived dentate gyrus granule cells

Katalin Vincze[1,2], Edit Hathy[1], Krisztina Pesti[3,4,5], Gergő Vőfély[2], Eszter Szabó[2], Csongor Tordai[1, 2], László Homolya[2], Zsófia Nemoda[1,6], Arpad Mike[3,7], Ágota Apáti[2], János M. Réthelyi[1,8]

1. Molecular Psychiatry Research Group, Semmelweis University, Balassa street 6, Budapest, 1083, Hungary
2. Institute of Molecular Life Sciences, HUN-REN Research Center for Natural Sciences, Magyar tudósok körútja 2, Budapest, 1117, Hungary
3. Opto-Neuropharmacology Group, Eötvös Loránd University, Department of Biochemistry, Pázmány Péter sétány 1/A, Budapest, 1117, Hungary
4. Department of Biological Resources, HUN-REN Centre for Agricultural Research, Brunszvik utca 2, Martonvásár, 2462, Hungary
5. Integrative Neuroendocrinology Research Group, HUN-REN Institute of Experimental Medicine, Szigony utca 43, Budapest, 1083, Hungary
6. Department of Molecular Biology, Semmelweis University, Tűzoltó u. 37-47, Budapest, 1094, Hungary
7. Department of Pharmacology and Drug Safety Research, Gedeon Richter Plc., Gyömrői út 19-21, Budapest, 1103, Hungary
8. Department of Psychiatry and Psychotherapy, Semmelweis University, Balassa street 6, Budapest, 1083, Hungary

**** Corresponding authors:***
Ágota Apáti
Institute of Molecular Life Sciences, HUN-REN Research Center for Natural Sciences
1117 Magyar tudósok körútja 2. Budapest, Hungary
Tel/Fax: +3613826607
Email: apati.agota@ttk.hu

János M. Réthelyi
Department of Psychiatry and Psychotherapy, Semmelweis University,
1083 Budapest, Balassa utca 6. Budapest, Hungary
Tel/Fax: +3612100336
Email: rethelyi.janos@semmelweis.hu

Author ORCIDs

Katalin Vincze https://orcid.org/0000-0002-4668-1134

Edit Hathy https: //orcid.org/0000-0001-8977-5686

Csongor Tordai https: //orcid.org/0000-0001-9770-997X

László Homolya https://orcid.org/0000-0003-1639-8140

Zsófia Nemoda https: //orcid.org/0000-0002-9550-7730

Arpad Mike https://orcid.org/0000-0002-9095-8161

Ágota Apáti https://orcid.org/0000-0003-0380-8139

János M. Réthelyi https://orcid.org/0000-0002-3641-012X

Abstract

Background

Nicotinic acetylcholine receptors (nAChRs) are expressed throughout the mammalian central nervous system, mediating cholinergic neurotransmission both in the developing and the adult brain. Among these, alpha 7 (α7) nAChRs demonstrate unique pharmacological properties and are potential targets in the treatment of neuropsychiatric disorders. α7nAChRs are also present in the hippocampus, therefore, we investigated this receptor type in human induced pluripotent stem cell (hiPSC) derived dentate gyrus (DG) granule cells, an *in vitro* model system of adult hippocampal neurogenesis.

Methods

DG granule cells were generated from hiPSCs to investigate the nAChR α7 subunit expression via qPCR, RNA-sequencing, and bungarotoxin-staining. To validate receptor function, we employed single-neuron patch-clamp electrophysiology. Calcium-imaging was used to assess spontaneous and ligand-evoked calcium-transients, while multi-electrode array (MEA) measurements were applied to evaluate network activity. Experiments involved choline (agonist), PNU-120596 (allosteric activator), and methyllaconitine (antagonist).

Results

Our results showed α7nAChRs in hiPSCs-derived PROX1 and MAP2 positive DG granule cells. Patch-clamp electrophysiology revealed that the selective agonist choline evoked inward currents, which were greatly augmented by PNU-120596. Methyllycaconitine inhibited these currents. Ca-imaging showed increased transients in response to both

choline and PNU-120596, which were blocked by methyllycaconitine. MEA recordings indicated increased bursting activity with choline, but not with PNU-120596.

Conclusion

Our results suggest that hiPSC-derived DG granule cells are amenable to functional assays to investigate α7nAChR function and pharmacology. This model system can serve for testing the receptor in a neuronal population relevant for several psychiatric disorders, including schizophrenia, anxiety disorders, and Alzheimer's disease.

Key words

human iPSC; neuronal differentiation; hippocampus; dentate gyrus; granule cells; α7nAChR, pharmacological characterization

Abbreviations

DG - dentate gyrus

hiPSC - human induced pluripotent stem cell

KCl - Potassium chloride

MEA - multielectrode array

MLA- methyllycaconitine

nAChR - nicotinic acetylcholine receptor

NPC – neuralonal progenitor cells

PNU-120596 - (1-(5-chloro-2,4-dimethoxy-phenyl)-3-(5-methyl-isoxazol-3-yl)-urea)

α7nAChR - α7 nicotinic acetylcholine receptor

Introduction

The alpha 7 nicotinic acetylcholine receptor (α7nAChR) belongs to the family of nicotinic acetylcholine receptors (nAChRs), a cys-loop receptor group based on structure. These receptors form ligand-gated ion channels that respond to the neurotransmitter acetylcholine (ACh) and are also activated by exogenous nicotine. Various types of nAChRs are present throughout the mammalian central nervous system, which participate in a wide range of presynaptic and postsynaptic neuronal activities by integrating the effects of endogenous cholinergic transmissions [1]. The α7nAChR forms a homopentameric structure containing five α7 subunits, which are encoded by the *CHRNA7* gene [1]. To achieve the active membrane structure, during receptor trafficking, NACHO [2] and RIC-3 chaperone proteins are essential molecular components [3]. The α7nAChRs are involved in neuronal maturation, integration into neuronal circuitry, synaptic transmission, and potentially play an important role in neurodegenerative and neuropsychiatric disorders, including Alzheimer's disease, anxiety disorders and schizophrenia [4-6].

The α7nAChR ion channel exhibits several unique features, including high calcium permeability, pronounced inward rectification, and rapid and reversible desensitization [7]. Electrophysiological measurements with the application of selective activators, inhibitors, and modulators allow a targeted functional characterization of α7nAChRs. Choline, a precursor and metabolite of ACh, acts as a selective agonist on α7nAChRs, while methyllycaconitine (MLA) is a selective receptor antagonist at low concentrations [8, 9]. Regarding pharmacological modulators, PNU-120596 is a selective, positive allosteric modulator, increasing agonist-induced peak currents and prolonging the evoked response.

Importantly, PNU-120596 has no effect on other neural nAChRs, such as α4β2, α3β4, and α9α10 [10]. Electrophysiological investigation of the rat α7nAChR has shown biphasic choline-evoked currents when modulated by PNU-12059 and allowed the assessment of peak open probability of choline-evoked currents [11]. Based on the non-selective channel activity, α7nAChR activation directly affects cytoplasmic Ca^{2+} levels through the high Ca^{2+} permeability of the ion channel, leading to further activation of voltage-dependent calcium channels, and Ca^{2+}-induced Ca^{2+} release (CICR) from the endoplasmic reticulum [12].

In this work, we focused on the analysis of the α7nAChRs in human induced pluripotent stem cell (hiPSC) derived hippocampal dentate gyrus (DG) granule cells. In humans, α7nAChR expression is predominant in brain areas associated with cognition and memory, including the amygdala, neocortex, and the basal forebrain (nucleus basalis Meyneri), and the hippocampus [13], mainly in the CA1, CA3, and the dentate gyrus [14]. The DG is a key area for memory formation and pattern recognition, associated with adult neurogenesis, i.e., the generation of new granule cells. DG cells receive input from the entorhinal cortex and project to the CA3 region of the hippocampus and have the unique feature of continuous neurogenesis even in adulthood. DG granule cells show long-term potentiation, the long-lasting strengthening of synaptic connections after repeated stimulation, the process implicated in learning [1, 15].

The α7nAChR plays an important role in neuronal maturation and integration [16] and the development of neurites [17, 18]. It has been described that receptor activation influences synaptic plasticity, neurogenesis, signal transduction, local excitability, neurotransmitter release, and has an impact on pattern separation and declarative memory [1]. The α7nAChR receptor may also be involved in cognitive dysfunction associated with

Alzheimer's disease and schizophrenia, based on animal models, whereas human studies did not confirm these findings unambiguously [19]. Interestingly, in addition to brain expression, α7nAChR is also present in a variety of immune cells, thus forming a potential correlated response of the neuro-immunological network [20].

An entirely human-specific negative regulator of α7nAChRs is *CHRFAM7A*, a hybrid gene resulting from a partial duplication and gene fusion between sequences of *CHRNA7* (exons 5-10) and *FAM7A*. The resulting protein's transmembrane and intracellular domains originate from *CHRNA7* [13], but it lacks the membrane trafficking signal and the agonist-binding site [21]. This fusion gene is present in 1-3 copies in most human individuals. Upregulation of *CHRNA7* showed an association with schizophrenia and bipolar disorder, while the low gene dosage and expression seem to have an association with Alzheimer's disease [13]. Additionally, it can be detected in two different orientations, either direct or inverted, the latter with a 2-bp deletion [13]. The presence of the inverted allele *CHRFAM7AΔ2bp* did not affect the α7nAChR channel opening [22]. This variant, however, shows an association with schizophrenia and specific endophenotypes such as episodic memory and P50 sensory gating deficiency [20].

Previous hiPSC-based studies investigating the human α7nAChRs *in vitro* have demonstrated several properties of the receptor [9, 13, 23, 24], however, the neuronal differentiation protocols used did not result in a specific neuronal population relevant for this receptor subtype. Directed differentiation of hiPSCs has become an outstanding tool in developmental neurobiology and neuropharmacology, with a unique opportunity to investigate specific human brain regions and neuronal populations involving selected receptor activation and complex signalling [25]. Our current work could pave the way to a

more detailed pharmacological characterization of this important receptor in the hippocampal DG granule cells, supporting drug discovery and development, and personalized approaches taking into account individual genetic differences. In the present work, our aim was to perform a molecular and functional characterization of the human α7AChRs in hippocampal DG granule cells generated from hiPSCs, using single-cell and multi-electrode electrophysiology in combination with pharmacological modulation and calcium imaging. The combined analysis of electrophysiology and cellular calcium transients allows a detailed functional analysis of this receptor subtype.

Materials and methods

Human iPSC lines

The healthy male control XCL-1 cell line was purchased from XCellScience (Novato, CAXIP-001-1V). hiPSC 62F was derived from fibroblasts obtained from a healthy male donor. The cell line was thankfully received from Professor Fred H. Gage (Salk Institute, United States).

Neuronal differentiation of hiPSC lines into DGGCs

From both XCL1 and 62F, neuronal progenitor cells (NPCs) were generated, following the protocol of Yu and colleagues [26] as published previously [27-29]. For further neuronal differentiation, the NPCs were plated onto a poly-ornithine/laminin-coated well in DMEM/F-12, GlutaMAX™ N2/B27 medium containing 20 ng/ml FGF2 (Thermo Fisher Scientific, MA, USA) and 1 µg/ml laminin. On the next day, the medium was switched to N2/B27 medium supplemented with 200 nM ascorbic acid (Sigma, MO, USA), 20 ng/ml BDNF (PeproTech,

NJ, USA), 500 µg/ml cAMP (Sigma, MO, USA), 1 µg/ml Laminin, and 20 ng/ml Wnt3A (Research and Diagnostic Systems Inc., MN, USA). After 3 weeks, Wnt3A was removed from the medium. The medium was changed every other day.

Immunostaining

The NPCs were seeded onto poly-ornithine/laminin-coated 8-well confocal chamber (Nunc Lab-Tek, Thermo Fisher Scientific). NPC marker staining was performed after 1 day of seeding, neuronal marker staining after 6 weeks of differentiation, following the previously described protocol (Hathy et al., 2020). Visualization of α7AChRs was carried out using Alexa Fluor™-conjugated alpha-Bungarotoxin (Thermo Fisher Scientific, MA, USA) according to the manufacturer's instructions. Immunofluorescence images were acquired using a Zeiss LSM 900 confocal laser-scanning microscope and processed with Zen software.

Gene expression measurement

For real-time quantitative PCR, RNA samples were prepared using Trizol (Thermo Fisher Scientific) according to the manufacturer's instructions. The samples were reverse transcribed into cDNA using AMV Reverse Transcriptase (Promega). The expression of alpha 7 was determined using a pre-developed TaqMan assay (Thermo Fisher Scientific, MA, USA). The PCR reactions were performed following the manufacturer's instructions, using the Step One Plus PCR device (Applied Biosystems).

Whole-cell single-neuron patch-clamp

hiPSC-derived dentate gyrus granule cells were tested for neuron-specific ion channels using the whole-cell patch-clamp technique. Measurements were performed with an Axopatch 200 B amplifier and the pClamp software (Molecular Devices, Sunnyvale, CA). Currents mediated by voltage-gated or ligand-gated channels were digitalized at 100 kHz and filtered at 10 kHz (Digidata 1322A, Molecular Devices). Recording pipettes were fabricated from borosilicate capillary glass (World Precision Instruments) using a P-87 micropipette puller (Sutter Instruments). Pipette resistances were between 2 and 4 MΩs. Recording pipettes were filled with intracellular solution containing 50 mM CsCl, 60 mM CsF, 10 mM NaCl, 10 mM HEPES, and 20 mM EGTA, 298 mOsm, pH 7.2. During the experiment, cells were bathed in continuously perfused extracellular solution (flow rate~100 ml/h) 140 mM NaCl, 5 mM KCl, 2 mM CaCl2, 1 mM MgCl2, 5 mM HEPES-Na, 10 mM D-glucose, 305 mOsm, pH 7.3. For fast drug application, we used a pressure-controlled dual U-tube system [30]. Solution exchange times were between 10 and 40 ms. Experiments were carried out at room temperature (~25°C). All chemical compounds were purchased from Sigma-Aldrich.

Ligand gated ion channel mediated currents were recorded at -70 mV. We tested GABA-, AMPA-, and α7nAChR receptor responses using GABA 10 μM, KA 100 μM, and Choline 10 mM as agonists (co-applied with 10 μM PNU-120596, a selective α7nAChR modulator). α7nAChR responses were inhibited by 1 μM MLA. The expression of functional voltage-gated sodium channels was tested using depolarizing steps from the holding potential of -120 to 60 mV in 10 mV increments. Steady-state inactivation was tested with 400 ms long voltage steps from -150 to -20 mV with 10 mV increments, followed by a 10 ms long

depolarizing voltage step to 0 mV. Average cell capacitances and series resistance values were 12.73 ± 4.12 pF and 6.18 ± 3.21 MΩ, respectively.

Calcium imaging

For calcium measurement, neuronal progenitor cells were seeded onto an 8-well confocal chamber that had been previously coated with poly-ornithine/laminin. Imaging was performed after 6 weeks of differentiation. The cytoplasmic calcium signals were evaluated using Fluo-4 AM calcium indicator dye as described previously (Pentek et al., 2016; Hathy et al., 2020). Reagents were purchased from Sigma or indicated otherwise. Baseline was recorded for 3–5 min before application of choline (40 μM or 4 mM), methyllycaconitine (MLA; 10 μM), PNU-120596 (4 μM), or potassium chloride (KCl; 50 mM). Cells were selected manually and marked as regions of interest (ROI) (29-300 neurons per recording). For analysis, we normalized the measured fluorescent intensity to the area. The baseline (F0) was determined using a Gaussian Mixture Model. Before stimulation, we collect the average fluorescence intensity values of the ROI at each time point. The distribution of these values is treated as a linear combination of normal distributions and is separated into normally distributed subpopulations. The number of subpopulations is determined by 10-fold cross-validation separately for each time series. The expected value of the distribution with the highest weight in the linear combination is chosen as the baseline. The reason for the choice of model is based on our assumption that the vast majority of data points cluster around the baseline level prior to stimulation, but a smaller, yet significant proportion of data points are located at a higher value due to spontaneous activity. To determine the maximum individual activity of the cells, the fluorescence intensity of each cell was characterized by the Fmax / F0 value, where Fmax is the highest fluorescence intensity measured during 50 frames after

administration, while F0 is the baseline activity of the cells recorded before administration, determined as stated above.

Statistical analysis

A statistical comparison was performed by comparing Fmax/F0 values of all measured cells, grouped by treatment condition. Each treatment condition was compared to the others. Data were assessed for normality using the Shapiro-Wilk test. As the distribution deviated from normality, the group comparisons were performed using a non-parametric Kruskal-Wallis test, followed by Dunn's post hoc test. The p-value < 0.0001 was considered to indicate statistical significance. The statistical analysis and visualization were performed in GraphPad Prism 8.0.2 software.

MEA measurements

Neuronal progenitors were transferred to poly-ornithine/laminin-coated 6-well MEA200/30iRTi chips (Multichannel Systems, MCS GmbH, Reutlingen, Germany), at a density of 100,000-150,000 cells/well. The day after seeding, we switched to differentiation medium and cultured the cells as described previously. The activity of the cultures was recorded twice a week, one day after the media change. Recordings were started after 5 minutes of acclimatization in the MEA setup. Baseline was recorded for 2–5 min before application of choline (40 µM) and PNU-120596 (4 µM).

Channels with excessive noise (above ±20µV) were excluded from the recording. Neuronal activity was recorded at a sampling rate of 20 kHz. The signal was filtered using a bandpass

filter with a frequency range of 300-3000 Hz. For data collection, the Multi Channel Experimenter, and for data processing, the Multi Channel Analyzer were used (Multichannel Systems, MCS GmbH, Reutlingen, Germany)

Results

DG granule cells are positive for neuronal markers and show spontaneous activity

Similar to previous experiments, we successfully generated SOX2 and Nestin positive NPCs **(Fig. 1A),** and taking these forward, MAP2 and PROX1 positive hiPSC-derived DG granule

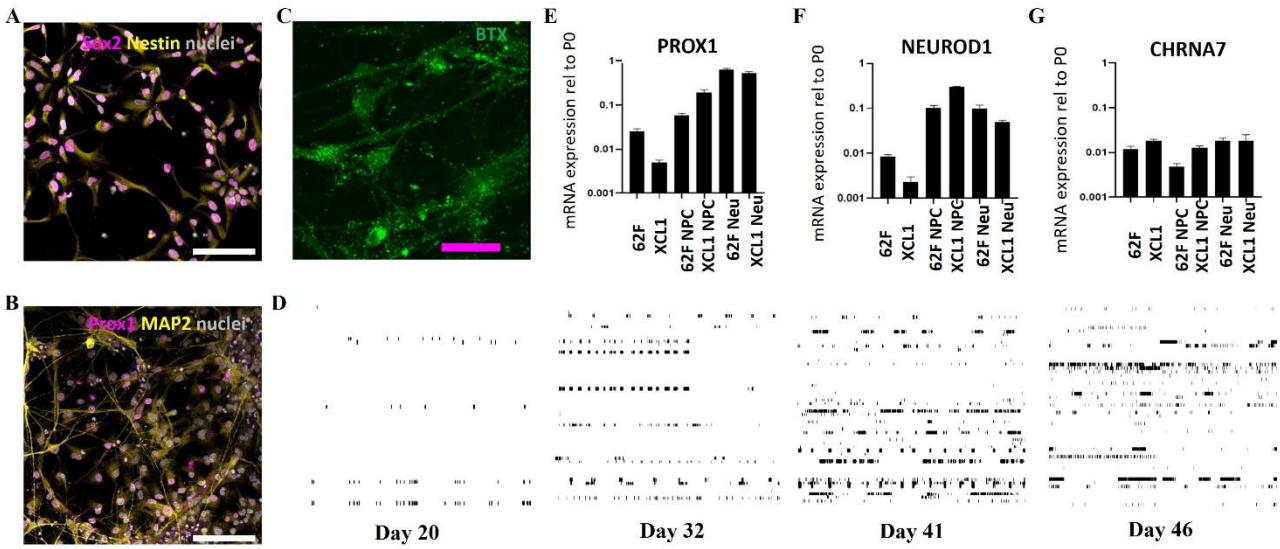


Figure 1. Characterization of 62F-derived DG granule cells.

(A) Representative immunocytochemistry image of 62F-derived NPC-s (SOX2-magenta and Nestin-yellow). The nuclei were counterstained by DAPI-grey (scale bar = 100 µm). (B) Representative immunocytochemistry image of the hiPSC-derived 41-days-old DG granule cells (MAP2-yellow and Prox1-magenta). The nuclei were counterstained by DAPI-gray (scale bar = 100 µm). (C) Bungarotoxin (BTX) immunostaining of the hiPSC-derived 41-days-old DG granule cells (scale bar = 50 µM). (D) Raster plots during differentiation of hiPSC-derived DG granule cells at day 20, 32, 41, and 46. Each row represents an electrode, and each vertical line represents a spike. (E-G) RT-PCR results showing mRNA expression levels of PROX1, NEUROD1, and CHRNA7 at pluripotent, NPC and neuronal stages for both cell lines.

cells **(Fig. 1B)** using two independent hiPSC lines. Moreover, the differentiated neurons stained positive with bungarotoxin, which is known to bind selectively to α7 nicotinic acetylcholine receptors **(Fig. 1C).** To validate the neurons' functionality, MEA measurements were performed, and the spontaneous electrical activity of neuronal cultures was investigated. Spiking and bursting activity was detectable from the 3rd week, increasing continuously, both in terms of the number of active electrodes, spike numbers, and intensity and duration, until day 40 day, when cultures reached synchronized activity, which was measurable even after 50 days **(Fig. 1D)**. We have assessed the expression of NEUROD1, PROX1, and CHRNA7 by qPCR at hiPSC, NPC, and neuronal stages in both cell lines **(Fig. 1E-G).** Neurons from both cell lines also demonstrated spontaneous activity measured as number of Ca-transients at week 6 **(Fig. 5C-F and Supp. Fig. 1A-C).** Both the synchronized electrical activity and the Ca-transients are indicative of functionally active synapses.

Patch-Clamp characterization of voltage-gated sodium channels and α7nAChRs in DG granule cells

Functional sodium channels were detected at 75 % of the cells (n = 38). A representative example shows the voltage-dependent activation and inactivation of sodium channels in a cell in **Fig. 2A-B**. Examples of sodium currents that had a peak amplitude > 1 nA upon depolarization to 0 mV are shown in **Fig. 2C** from 12 different cells. Summary of peak amplitude data using the activation and inactivation protocols is shown in **Fig. 2D.** Examples for ligand gated ion channel mediated responses are shown in **Fig. 3** and **Supp. Fig. 2A-B.**

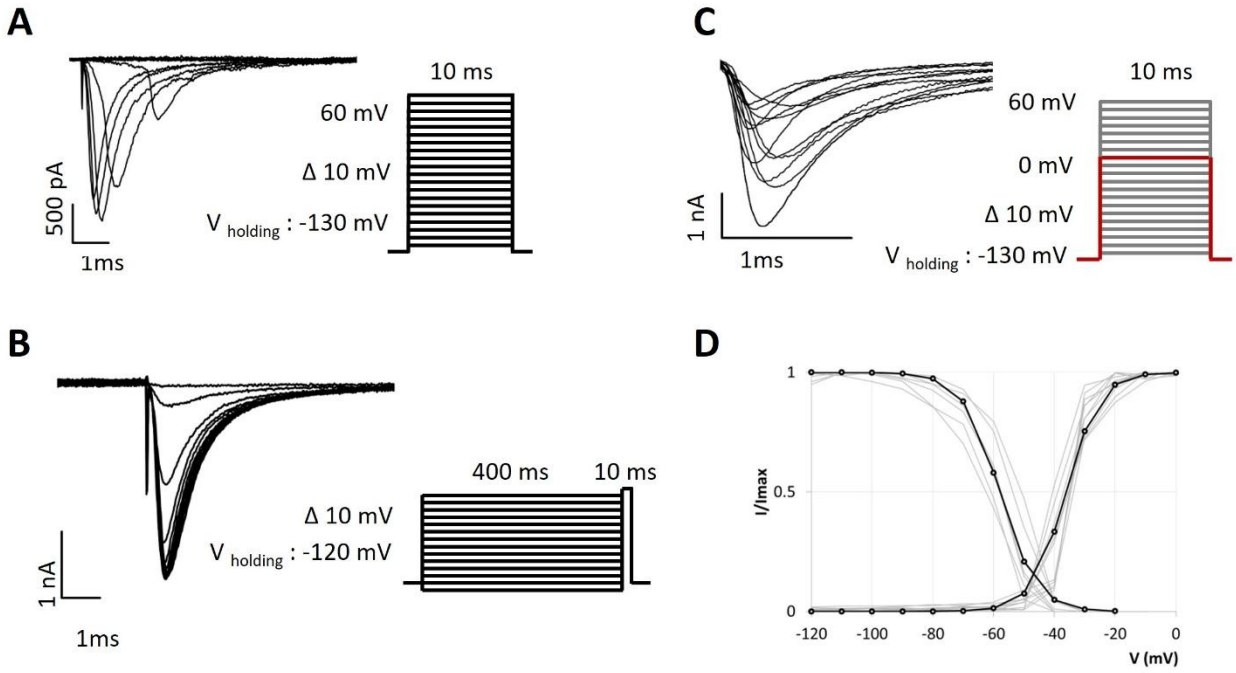


Figure 2. Sodium currents in hiPSC-derived DG granule cells are hiPSC-derived DG granule cells cells evoked by voltage steps. (A-C) Insets show the applied voltage protocol. (A) Example for sodium currents in a cell by the activation protocol. (B) Example for sodium currents evoked by the inactivation protocol. (C) Sodium currents evoked by voltage steps to 0 mV from 12 individual cells. (D) Plots of sodium current activation and inactivation. Grey lines indicate measurements from individual cells. Individual curves were fitted by the Boltzmann equation. Half-activation and half-inactivation voltages ($V_{1/2}$) and slope factors (k) were averaged. Black lines show reconstructed curves using the average $V_{1/2}$ and k parameters.

50 % of the cells responded to 100 μM kainate, 66 % to 10 μM GABA, and 41 % to 10 mM choline together with the positive modulator PNU-120596.

Using single-cell electrophysiology we could characterize α7nAChRs-associated LGICs in DG granule cells. We found that choline and PNU-120596, administered together, activated an inward current, but not PNU-120596 alone (**Fig. 3A**). Choline alone evoked a small

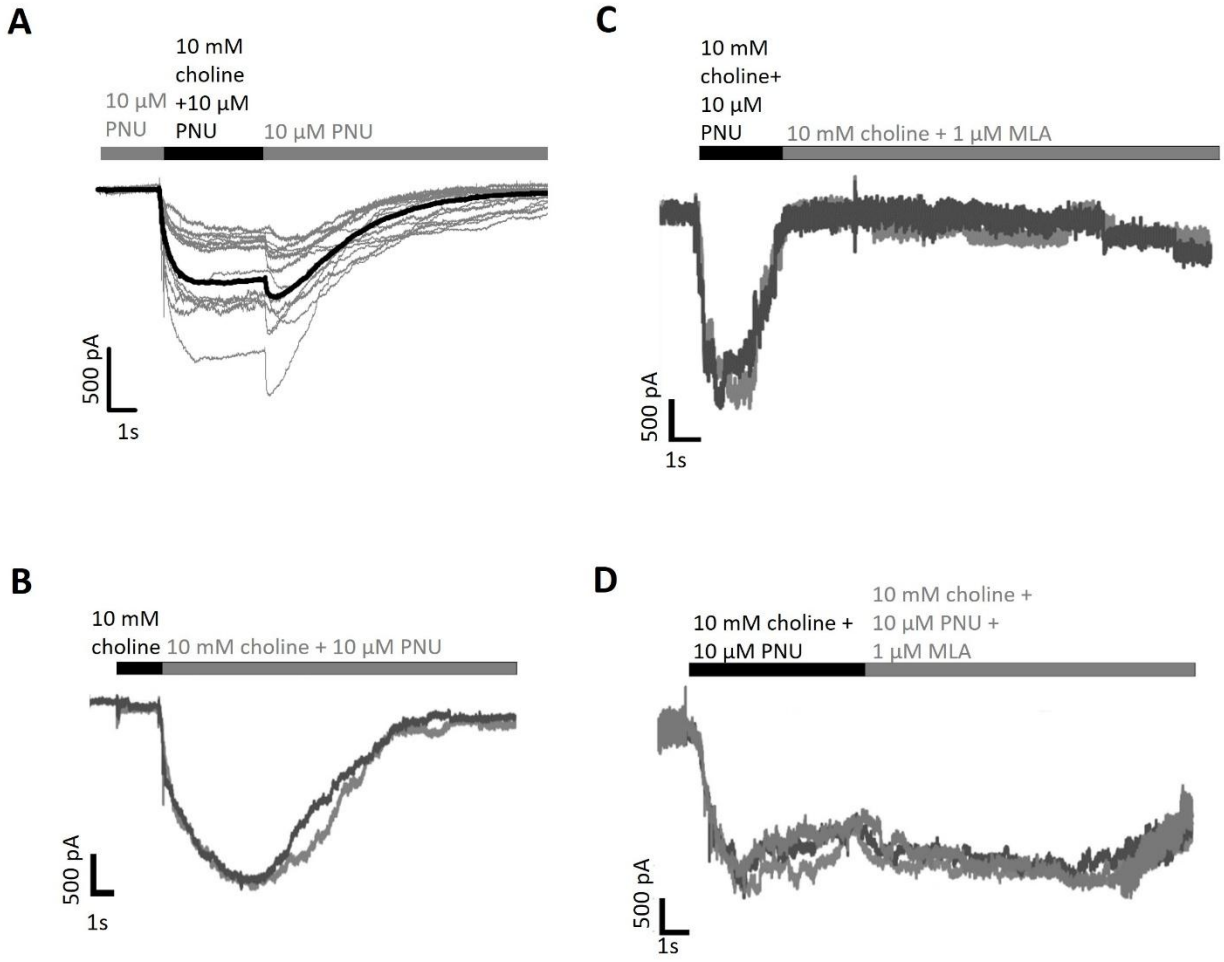


Figure 3. **Ionic currents evoked by pharmacological agents acting on alpha7 nAChRs.**

(A) Alpha7 nAChR mediated currents evoked by PNU alone (grey bar) and choline+PNU (black bar). (B) Currents evoked by choline alone (black bar) and choline+PNU (grey bar). (C) Currents evoked by choline+PNU (black bar) and choline+MLA (grey bar). (D) Currents evoked by choline+PNU (black bar) and choline+PNU+MLA (grey bar). Bars above the charts indicate the length of agonist pulses. LGIC currents were recorded at -70 mV. The following concentrations were used: choline - 10 mM, PNU-12596 – 10 μM, MLA – 1 μM.

transient current **(Fig. 3B)**. MLA, when co-applied with choline, inhibited the current evoked by co-applied choline and PNU-120596 (**Fig. 3C**) but failed to inhibit the current in the continuing presence of PNU-120596 (**Fig. 3D**).

The effects of α7nAChRs activation on DG granule cell network activity

We observed spontaneous activity from the 20th day onwards **(Fig. 1D)**. The detected spike pattern evolved during differentiation; spikes were arranged in periodically occurring bursts, which involved multiple electrodes **(Fig. 4 A, E, I, and C, G, K).** After choline administration (40 μM), we observed altered, continuous activity on multiple electrodes **(Fig. 4 B, F)**, and the overall activation pattern of the culture became disorganized **(Fig. 4 J)**. Following PNU-120596 administration, we observed changes in individual electrode activity **(Fig. 4D, H)**, while the overall activity of the culture remained similar. **(Fig 4 L).**

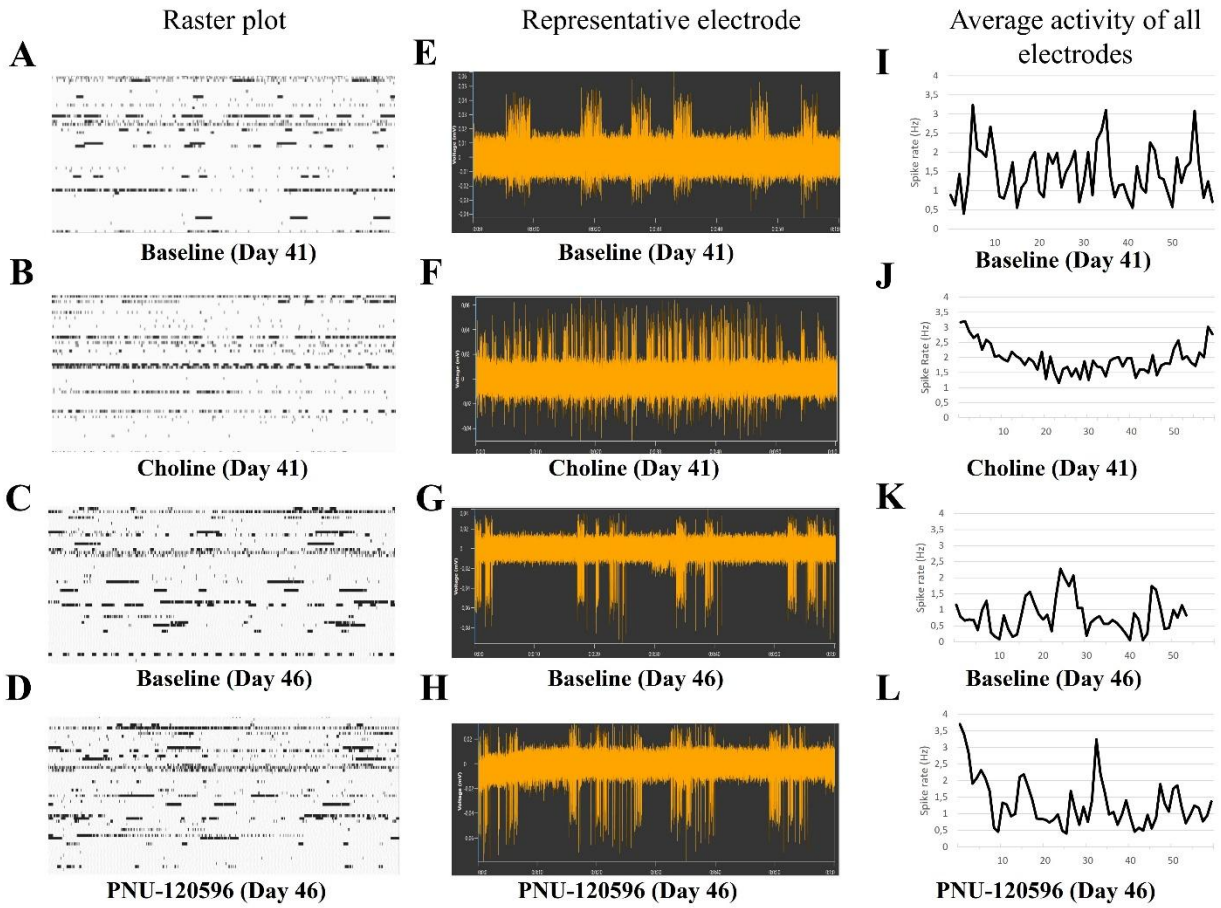


Figure 4. Electrical activity of hippocampal 62F-derived neurons during differentiation and in response to choline and PNU120596. Representative raster plots (A, B, C, D) where each row represents an electrode, and each vertical line represents a spike; the measurement time is one minute. Representative single-electrode recordings (E,F,G,H) and Spike Rate (Hz) graphs (I,J,K,L) shows the average number of spikes per second, across all active electrodes. Spontaneous activity (A, E, I) and response to choline (B, F, J) at 41 days of differentiation. Spontaneous activity (C, G, K) and response to PNU-120596 (D, H, L) at 46 days of differentiation.

Calcium-imaging measurements of α7nAChRs function

To further test the functional activity and network properties of α7nAChRs, we performed calcium imaging measurements. The majority of differentiated Fluo-4-AM-loaded cells exhibited neural morphology (**Fig. 5A-B and Supp. Fig. 3A- B),** spontaneous Ca-transients, and inducible Ca-signals **(Fig. 5C-F and Supp. Fig. 3C-E)** in both cell lines. We observed

that a low concentration of choline (40 µM) was not sufficient to provoke significant fluorescence intensity changes **(Fig. 5C and Supp. Fig. 3C)**; at higher concentrations (4 mM), choline influenced the cultures' activity **(Fig. 5F)**, although not at a level to provoke

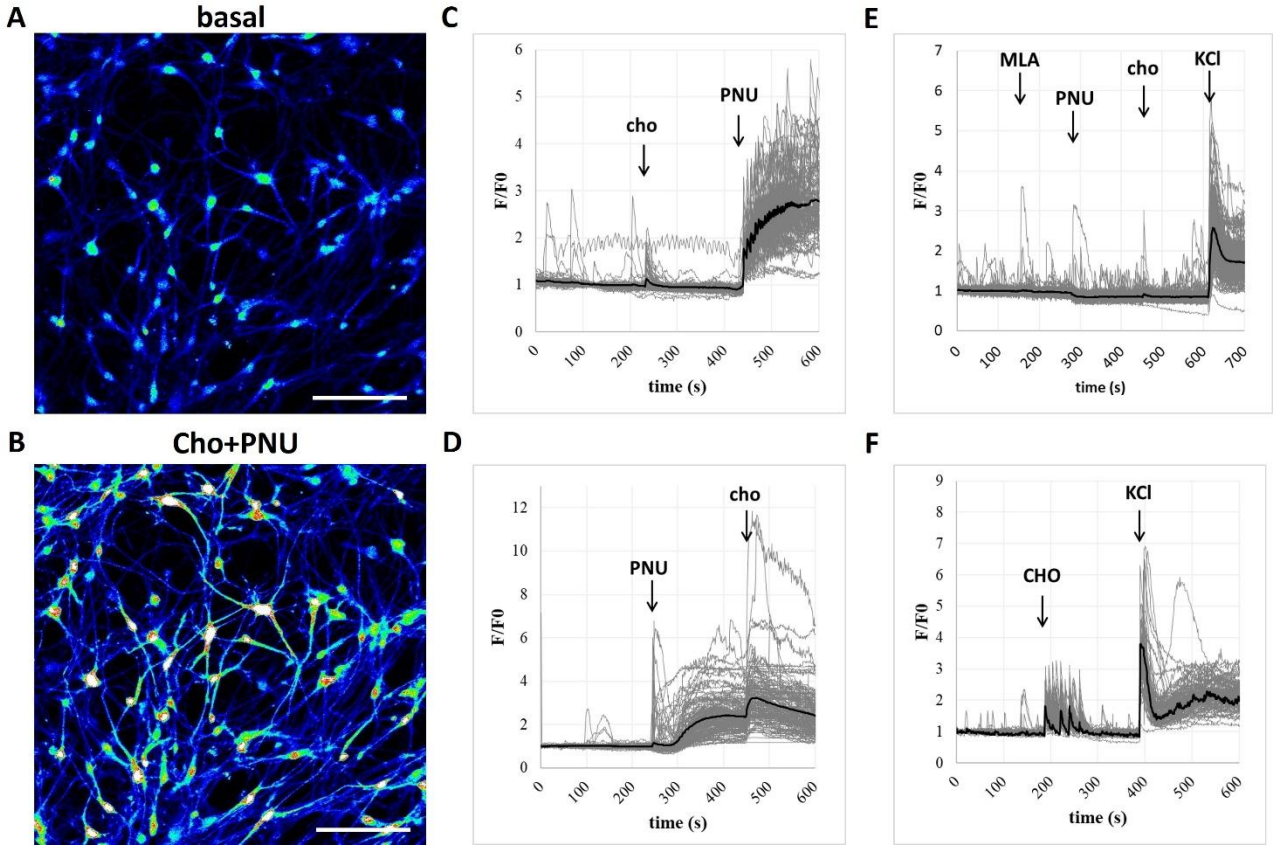


Figure 5. Alterations in calcium transients after treatment with pharmacological agents acting on alpha7 nAChRs. (A-B) Representative confocal microscopy images were obtained, and calcium signals were measured in Fluo-4 loaded 62F-derived neurons, before (A) and after (B) addition of choline and PNU-120596. (scale bar = 100 µM, artificial colouring) (C) Choline alone elicits subtle changes in calcium transients; however, after the addition of PNU-120596, calcium activity increased dramatically. (D) PNU-120596 alone can evoke calcium transients in neurons that are further increased by the addition of choline. (E) MLA abolishes the effects of both PNU-120596 alone and PNU-120596+choline. (F) High-dose choline elicits an observable but transient calcium-wave. Abbreviations: cho: Choline (40 µM), CHO: Choline (4 mM), MLA: methyllycaconitine (10 µM), PNU: PNU-120596 (4 µM), KCl: Potassium chloride, 50 mM, F/F0: Fluorescence intensity normalised to baseline activity

significant increases in fluorescence levels **(Fig. 6)**. However, after PNU-120596 (4 µM) administration, choline had a strong effect on intensity and frequency of calcium-signals **(Fig. 5D and Supp. Fig. 3D)**. Interestingly, PNU-120596 alone increased calcium-

transients, suggestive of the presence of an endogenous agonist of α7nAChR or an intrinsic metabotropic effect of PNU-120596. After MLA administration, neither PNU-120596 nor choline was able to induce changes in fluorescence levels in the cultures **(Fig. 5E and Supp. Fig. 3E)**. As the resulting response was completely abolished by adding MLA, a selective α7nAChR antagonist, it was proven that the choline-evoked calcium waves were activated by α7nAChR. It is worth noting that significant Ca-transients were measured upon the depolarizing effect of KCl **(Fig. 5E-F and Supp. Fig. 3E)**. Corresponding Ca-measurements were obtained in both tested cell lines, which were analyzed and showed that PNU-120596, PNU-120596+choline, and KCl significantly increased the basal Ca level in the cells **(Fig. 6. and Supp. Fig. 3F).**

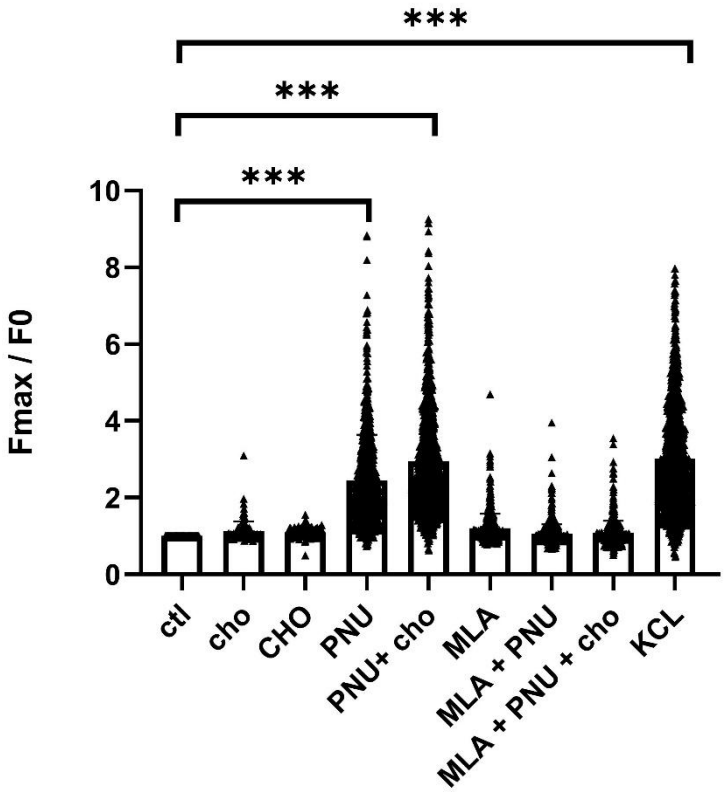


Figure 6. Overall intensity changes in calcium fluorescence after addition of different alpha7 nAChR pharmacological agents and KCl.

The bar graph shows the change in maximum intensity of each cell in response to a given treatment, after 41 days of differentiation, of hiPS-62F-derived neurons calculated from 2-7 biological parallels. Each triangle represents one cell (N=130-1300). Fmax/F0 fluorescent intensities were calculated by determining average basal activity(F0) and maximal values (Fmax) after the indicated treatments. For statistical comparison between subjects, the Kruskal-Wallis test was performed.

Discussion

Human iPSC-based disease modeling has developed into an important approach in neurobiology, disease modelling, and neuropharmacology. With the advent of somatic cell reprogramming and specific neuronal differentiation protocols, it is now possible to generate specific, disease-relevant neuronal cultures from healthy and diseased individuals. Moreover, this model system represents a unique opportunity to investigate neuronal cells of specific temporal and spatial identities *in vitro* using various methodological approaches, including pharmacological characterization.

In the present work, we generated hippocampal DG granule cells via an established protocol [26], which gives rise to these hippocampal neurons by faithfully recapitulating adult neurogenesis in the dentate gyrus. We have investigated the expression, function, and pharmacological properties of the α7nAChRs in this neuronal population relevant for several psychiatric disorders, including schizophrenia, anxiety disorders, and Alzheimer's disease.

The α7 type of nACh receptor is found in a large variety of neuronal and immune cells and has a particular importance in human cognition and related diseases. The activation of the receptor initiates calcium influx (both directly and indirectly), increases neuronal excitability, and promotes neurotransmitter release. α7nAChR activation can also influence inflammation, autophagy, and apoptosis, mainly through JAK/STAT and AMPK pathways. It has a neuroprotective effect, mediating its action primarily through the PI3K/Akt and NF-κB pathways [12]. Therefore, the pharmacological modulation of α7nAChRs, especially in the

area of the hippocampus, may serve as an important treatment approach for the related disorders.

Based on animal and human studies, the main nAChR populations in the hippocampus are α4β2 and α7 [31]. In accordance with these data, we have confirmed by qPCR mRNA-level expression of the CHRNA7 gene, coding the subunit of the homopentameric receptor in the hippocampal DG granule cells. At the protein level, the presence of the receptor in the cell membrane cannot be reliably determined by immunocytochemistry, as most commercially available antibodies also recognize the monomer CHRNA7 subunit inside the cells, and do not provide information whether the subunits indeed properly fold and are trafficked to the membrane and form the homopentameric, functionally active α7 receptor. In this work, for cell surface receptor visualization we used bungarotoxin, which selectively binds to the α7 subunit on the membrane [32], while only functional studies can ascertain proper α7nAChR function.

To validate the presence of the functional α7nAChRs in the DG granule cells, we have used selective ligands, modulators, and inhibitors of the receptor. Choline, a metabolite and precursor of ACh acts as a full agonist on α7nAChRs; while its effect varies and is weaker on other nAchRs [33, 34]. PNU-120596 is a positive allosteric modulator of α7nAChRs, which, since it may greatly increase the activation of α7nAChRs in the presence of acetylcholine, has been considered a potential drug to enhance cholinergic therapies [35]. Here, we found that the combination of choline and PNU-120596 increases α7nAChR single-cell current and activates the calcium transients in the DG granule cells. This is in line with the related data in the literature [36], showing that by enhancing α7nAChRs receptor activation, PNU-120596 increases secondary ryanodine receptor-driven CICR and inositol-induced calcium release. In this study, we have seen a small effect of PNU-120596 on

calcium transients even in the absence of added choline, but the presence of choline at low levels in the culture medium cannot be excluded.

Importantly, in our experiments, the choline + PNU-120596 dependent changes in both DG granule cell membrane potential and the activation of the calcium transients were strongly inhibited by MLA, a selective α7nAChRs receptor inhibitor. Taken together, these data strongly indicate the functional presence of α7nAChRs in human hiPSC-derived hippocampal DG granule cells, and the possibility to use these preparations for future pharmacological studies.

The importance of using human cell-based systems for *in vitro* studies is underlined by the presence of a human-specific negative regulator protein of α7nAChRs, CHRFAM7A. A late evolutionary product in the human genome, the *CHRFAM7A* gene is translated into the dupα7 protein, which can be inserted into the α7nAChR pentamer, producing a modified, lower channel activity version of the receptor [20]. The presence of dupα7 was shown to influence the kinetics of the receptor activation and its desensitization in the presence of PNU-120596 [13]. Moreover, the presence of this transcript has been confirmed in several brain regions, including the hippocampus, and the *CHRFAM7A* gene polymorphisms are suggested to be associated with certain psychiatric and neurological disorders [20, 37, 38].

The pharmacological modulation of α7nAChRs may have a special importance in human diseases related to neuronal, especially cognitive and behavioral functions. In Alzheimer's disease, the activation of this receptor has been linked to the reduction of certain symptoms [2]. It has been reported that the α7nAChR and amyloid beta (Aβ) co-localize in the hippocampal neurons [39]. In a model system, increased α7 receptor expression was

associated with increased cellular (Aβ1-42) uptake, and the addition of the receptor inhibitor MLA reduced Aβ accumulation [39].

In schizophrenia, analysis of post-mortem samples revealed that certain areas of the hippocampus express low α7nAChRs protein levels, although the possible impact of long-term antipsychotic medication on this finding needs to be considered [40]. However, Leonard and colleagues detected several mutations in the promoter region of CHRNA7 that negatively affect the expression of the gene. The presence of those polymorphisms was statistically higher in schizophrenia patients than in controls [41]. In case of recent-onset schizophrenia patients, lower α7nAChR levels were found to associate with positive symptoms and poorer cognitive performance [42]. Genome-wide surveys suggested that changes in gene copy numbers are associated with the risk of schizophrenia [6].

In summary, our overall objective was the molecular and functional characterization of α7nAChRs in hiPSC-derived dentate gyrus granule cells. We used molecular, morphological, electrophysiological, and calcium-imaging methodologies to assess the function of this receptor subtype in this novel human neuronal model system. Our results provide proof-of-concept for using this *in vitro* human cell-based model system for further experiments investigating receptor subtypes and neuronal cell lines derived from diseased individuals. Moreover, our methods represent a window of opportunity for genetically informed, personalized, precision-medicine approaches.

Funding statement

Funding of this study was provided by the Hungarian Brain Research Program (Nemzeti Agykutatási Program, NAP) grants KTIA_NAP_13-2014-0011 and 2017-1.2.1-NKP-2017-00002 to JRM, KTIA-NAP-13-2-2014-002 to AM, and NAP-A KTIA_13_NAP-A-I/6 to ÁA and LH, GINOP-2.1.1-15-2015-00369 to ÁA, and the National Research Development and Innovation Office grants NKFIH K129195 and TKP2021-EGA-25 to JMR.

The authors would like to thank Beáta Haraszti, Réka Gárdos, and Márton Széphalmi for their technical assistance and Balázs Sarkadi for his useful advice during the preparation of the manuscript. We are grateful for hiPSC 62F line received from Professor Fred H. Gage.

Ethics declarations

Ethics approval and consent to participate

Generation of iPSC lines, and all downstream assays were approved by the Human Reproduction Committee of the Hungarian Health Science Council (ETT HRB). All participants gave written informed consent.

Competing interests

Katalin Vincze is a full-time employee of Salus Kft, Budapest, Hungary. However, Salus Kft had no role in the planning, executing, interpreting, or discussing the results of this communication. Gergő Vőfély and Arpad Mike are currently employed by Richter Gedeon

Plc. not affecting the content of this manuscript. The authors declare no other competing financial or non-financial interests.

Author contributions

KV: conceptualization, investigation methodology, project administration, visualization, writing –original draft; AM, LH, ZN, AÁ, JMR: conceptualization, formal analysis, funding acquisition, methodology, resources, supervision, and writing - Original Draft and Review & Editing; EH, KP, GV, CT, ES: investigation, methodology, validation, visualization. All authors have contributed to and approved the manuscript.

References

[1] Letsinger AC, Gu Z, Yakel JL. alpha7 nicotinic acetylcholine receptors in the hippocampal circuit: taming complexity. Trends Neurosci. 2022;45:145-57.

[2] Gu S, Matta JA, Lord B, Harrington AW, Sutton SW, Davini WB, et al. Brain alpha7 Nicotinic Acetylcholine Receptor Assembly Requires NACHO. Neuron. 2016;89:948-55.

[3] Williams ME, Burton B, Urrutia A, Shcherbatko A, Chavez-Noriega LE, Cohen CJ, et al. Ric-3 promotes functional expression of the nicotinic acetylcholine receptor alpha7 subunit in mammalian cells. J Biol Chem. 2005;280:1257-63.

[4] Letsinger AC, Nacer SA, Stevanovic KD, Larson GJ, DeFilipp JS, Cushman JD, et al. Genetic deletion of alpha7 nAChRs reduces hippocampal granule and pyramidal cell number in both sexes but impairs pattern separation in males only. Front Neurosci. 2023;17:1244118.

[5] Hernandez CM, Dineley KT. alpha7 nicotinic acetylcholine receptors in Alzheimer's disease: neuroprotective, neurotrophic or both? Curr Drug Targets. 2012;13:613-22.

[6] Thomsen MS, Weyn A, Mikkelsen JD. Hippocampal alpha7 nicotinic acetylcholine receptor levels in patients with schizophrenia, bipolar disorder, or major depressive disorder. Bipolar Disord. 2011;13:701-7.

[7] Papke RL, Horenstein NA. Therapeutic Targeting of alpha7 Nicotinic Acetylcholine Receptors. Pharmacol Rev. 2021;73:1118-49.

[8] Mike A, Castro NG, Albuquerque EX. Choline and acetylcholine have similar kinetic properties of activation and desensitization on the alpha7 nicotinic receptors in rat hippocampal neurons. Brain Res. 2000;882:155-68.

[9] Larsen HM, Hansen SK, Mikkelsen JD, Hyttel P, Stummann TC. Alpha7 nicotinic acetylcholine receptors and neural network synaptic transmission in human induced pluripotent stem cell-derived neurons. Stem Cell Res. 2019;41:101642.

[10] Hurst RS, Hajos M, Raggenbass M, Wall TM, Higdon NR, Lawson JA, et al. A novel positive allosteric modulator of the alpha7 neuronal nicotinic acetylcholine receptor: in vitro and in vivo characterization. J Neurosci. 2005;25:4396-405.

[11] Szabo AK, Pesti K, Mike A, Vizi ES. Mode of action of the positive modulator PNU-120596 on alpha7 nicotinic acetylcholine receptors. Neuropharmacology. 2014;81:42-54.

[12] Xu ZQ, Zhang WJ, Su DF, Zhang GQ, Miao CY. Cellular responses and functions of alpha7 nicotinic acetylcholine receptor activation in the brain: a narrative review. Ann Transl Med. 2021;9:509.

[13] Ihnatovych I, Nayak TK, Ouf A, Sule N, Birkaya B, Chaves L, et al. iPSC model of CHRFAM7A effect on alpha7 nicotinic acetylcholine receptor function in the human context. Transl Psychiatry. 2019;9:59.

[14] Ma KG, Qian YH. Alpha 7 nicotinic acetylcholine receptor and its effects on Alzheimer's disease. Neuropeptides. 2019;73:96-106.

[15] Tirone F, Farioli-Vecchioli S, Micheli L, Ceccarelli M, Leonardi L. Genetic control of adult neurogenesis: interplay of differentiation, proliferation and survival modulates new neurons function, and memory circuits. Front Cell Neurosci. 2013;7:59.

[16] John D, Shelukhina I, Yanagawa Y, Deuchars J, Henderson Z. Functional alpha7 nicotinic receptors are expressed on immature granule cells of the postnatal dentate gyrus. Brain Res. 2015;1601:15-30.

[17] Nordman JC, Kabbani N. An interaction between alpha7 nicotinic receptors and a G-protein pathway complex regulates neurite growth in neural cells. J Cell Sci. 2012;125:5502-13.

[18] King JR, Kabbani N. Alpha 7 nicotinic receptors attenuate neurite development through calcium activation of calpain at the growth cone. PLoS One. 2018;13:e0197247.

[19] Lewis AS, van Schalkwyk GI, Bloch MH. Alpha-7 nicotinic agonists for cognitive deficits in neuropsychiatric disorders: A translational meta-analysis of rodent and human studies. Prog Neuropsychopharmacol Biol Psychiatry. 2017;75:45-53.

[20] Ihnatovych I, Saddler RA, Sule N, Szigeti K. Translational implications of CHRFAM7A, an elusive human-restricted fusion gene. Mol Psychiatry. 2024;29:1020-32.

[21] Gorgulu I, Jagannath V, Pons S, Koniuszewski F, Groszer M, Maskos U, et al. The human-specific nicotinic receptor subunit CHRFAM7A reduces alpha7 receptor function in human induced pluripotent stem cells-derived and transgenic mouse neurons. Eur J Neurosci. 2024;60:4893-906.

[22] Szigeti K, Ihnatovych I, Birkaya B, Chen Z, Ouf A, Indurthi DC, et al. CHRFAM7A: A human specific fusion gene, accounts for the translational gap for cholinergic strategies in Alzheimer's disease. EBioMedicine. 2020;59:102892.

[23] de Lucas-Cerrillo AM, Maldifassi MC, Arnalich F, Renart J, Atienza G, Serantes R, et al. Function of partially duplicated human alpha77 nicotinic receptor subunit CHRFAM7A gene: potential implications for the cholinergic anti-inflammatory response. J Biol Chem. 2011;286:594-606.

[24] Lasala M, Corradi J, Bruzzone A, Esandi MDC, Bouzat C. A human-specific, truncated alpha7 nicotinic receptor subunit assembles with full-length alpha7 and forms functional receptors with different stoichiometries. J Biol Chem. 2018;293:10707-17.

[25] Dutan Polit L, Eidhof I, McNeill RV, Warre-Cornish KM, Yde Ohki CM, Walter NM, et al. Recommendations, guidelines, and best practice for the use of human induced pluripotent stem cells for neuropharmacological studies of neuropsychiatric disorders. Neurosci Appl. 2023;2:101125.

[26] Yu DX, Di Giorgio FP, Yao J, Marchetto MC, Brennand K, Wright R, et al. Modeling hippocampal neurogenesis using human pluripotent stem cells. Stem Cell Reports. 2014;2:295-310.

[27] Tordai C, Hathy E, Gyergyak H, Vincze K, Baradits M, Koller J, et al. Probing the biological consequences of a previously undescribed de novo mutation of ZMYND11 in a schizophrenia patient

by CRISPR genome editing and induced pluripotent stem cell based in vitro disease-modeling. Schizophr Res. 2024;273:107-20.

[28] Vofely G, Berecz T, Szabo E, Szebenyi K, Hathy E, Orban TI, et al. Characterization of calcium signals in human induced pluripotent stem cell-derived dentate gyrus neuronal progenitors and mature neurons, stably expressing an advanced calcium indicator protein. Mol Cell Neurosci. 2018;88:222-30.

[29] Hathy E, Szabo E, Varga N, Erdei Z, Tordai C, Czehlar B, et al. Investigation of de novo mutations in a schizophrenia case-parent trio by induced pluripotent stem cell-based in vitro disease modeling: convergence of schizophrenia- and autism-related cellular phenotypes. Stem Cell Res Ther. 2020;11:504.

[30] Szasz BK, Mike A, Karoly R, Gerevich Z, Illes P, Vizi ES, et al. Direct inhibitory effect of fluoxetine on N-methyl-D-aspartate receptors in the central nervous system. Biol Psychiatry. 2007;62:1303-9.

[31] Yakel JL, Shao Z. Functional and molecular characterization of neuronal nicotinic ACh receptors in rat hippocampal interneurons. Prog Brain Res. 2004;145:95-107.

[32] Chen D, Patrick JW. The alpha-bungarotoxin-binding nicotinic acetylcholine receptor from rat brain contains only the alpha7 subunit. J Biol Chem. 1997;272:24024-9.

[33] Pereira EF, Hilmas C, Santos MD, Alkondon M, Maelicke A, Albuquerque EX. Unconventional ligands and modulators of nicotinic receptors. J Neurobiol. 2002;53:479-500.

[34] Gonzalez-Rubio JM, Rojo J, Tapia L, Maneu V, Mulet J, Valor LM, et al. Activation and blockade by choline of bovine alpha7 and alpha3beta4 nicotinic receptors expressed in oocytes. Eur J Pharmacol. 2006;535:53-60.

[35] Gusev AG, Uteshev VV. Physiological concentrations of choline activate native alpha7-containing nicotinic acetylcholine receptors in the presence of PNU-120596 [1-(5-chloro-2,4-dimethoxyphenyl)-3-(5-methylisoxazol-3-yl)-urea]. J Pharmacol Exp Ther. 2010;332:588-98.

[36] King JR, Ullah A, Bak E, Jafri MS, Kabbani N. Ionotropic and Metabotropic Mechanisms of Allosteric Modulation of alpha7 Nicotinic Receptor Intracellular Calcium. Mol Pharmacol. 2018;93:601-11.

[37] Sinkus ML, Graw S, Freedman R, Ross RG, Lester HA, Leonard S. The human CHRNA7 and CHRFAM7A genes: A review of the genetics, regulation, and function. Neuropharmacology. 2015;96:274-88.

[38] Di Lascio S, Fornasari D, Benfante R. The Human-Restricted Isoform of the alpha7 nAChR, CHRFAM7A: A Double-Edged Sword in Neurological and Inflammatory Disorders. Int J Mol Sci. 2022;23.

[39] Yang WN, Ma KG, Chen XL, Shi LL, Bu G, Hu XD, et al. Mitogen-activated protein kinase signaling pathways are involved in regulating α7 nicotinic acetylcholine receptor-mediated amyloid-β uptake in SH-SY5Y cells. Neuroscience. 2014;278:276-90.

[40] Young JW, Geyer MA. Evaluating the role of the alpha-7 nicotinic acetylcholine receptor in the pathophysiology and treatment of schizophrenia. Biochem Pharmacol. 2013;86:1122-32.

[41] Leonard S, Gault J, Hopkins J, Logel J, Vianzon R, Short M, et al. Association of promoter variants in the alpha7 nicotinic acetylcholine receptor subunit gene with an inhibitory deficit found in schizophrenia. Arch Gen Psychiatry. 2002;59:1085-96.

[42] Wong NR, Rubin LH, Harrington CK, Jenkins KR, Shinehouse LK, Yoon M, et al. Hippocampal Availability of the alpha7 Nicotinic Acetylcholine Receptor in Recent-Onset Psychosis. JAMA Netw Open. 2024;7:e2427163.

Figure captions

Figure 1. Characterization of 62F-derived DG granule cells.

(A) Representative immunocytochemistry image of 62F-derived NPC-s (SOX2-magenta and Nestin-yellow). The nuclei were counterstained by DAPI-grey (scale bar = 100 μm). (B) Representative immunocytochemistry image of the hiPSC-derived 41-days-old DG granule cells (MAP2-yellow and Prox1-magenta). The nuclei were counterstained by DAPI-gray (scale bar = 100 μm). (C) Bungarotoxin (BTX) immunostaining of the hiPSC-derived 41-days-old DG granule cells (scale bar = 50 μM). (D) Raster plots during differentiation of hiPSC-derived DG granule cells at day 20, 32, 41, and 46. Each row represents an electrode, and each vertical line represents a spike. (E-G) RT-PCR results showing mRNA expression levels of PROX1, NEUROD1, and CHRNA7 at pluripotent, NPC and neuronal stages for both cell lines.

Figure 2. Sodium currents in hiPSC-derived DG granule cells are hiPSC-derived DG granule cells cells evoked by voltage steps.

(A-C) Insets show the applied voltage protocol. (A) Example for sodium currents in a cell by the activation protocol. (B) Example for sodium currents evoked by the inactivation protocol. (C) Sodium currents evoked by voltage steps to 0 mV from 12 individual cells. (D) Plots of sodium current activation and inactivation. Grey lines indicate measurements from individual cells. Individual curves were fitted by the Boltzmann equation. Half-activation and half-inactivation voltages ($V_{1/2}$) and slope factors (k) were averaged. Black lines show reconstructed curves using the average $V_{1/2}$ and k parameters.

Figure 3. **Ionic currents evoked by pharmacological agents acting on alpha7 nAChRs.**

(A) Alpha7 nAChR mediated currents evoked by PNU alone (grey bar) and choline+PNU (black bar). (B) Currents evoked by choline alone (black bar) and choline+PNU (grey bar). (C) Currents evoked by choline+PNU (black bar) and choline+MLA (grey bar). (D) Currents evoked by choline+PNU (black bar) and choline+PNU+MLA (grey bar). Bars above the charts indicate the length of agonist pulses. LGIC currents were recorded at -70 mV. The following concentrations were used: choline - 10 mM, PNU-12596 – 10 μM, MLA – 1 μM.

Figure 4. Electrical activity of hippocampal 62F-derived neurons during differentiation and in response to choline and PNU120596.

Representative raster plots (A, B, C, D) where each row represents an electrode, and each vertical line represents a spike; the measurement time is one minute. Representative single-electrode recordings (E,F,G,H) and Spike Rate (Hz) graphs (I,J,K,L) shows the average number of spikes per second, across all active electrodes. Spontaneous activity (A, E, I) and response to choline (B, F, J) at 41 days of differentiation. Spontaneous activity (C, G, K) and response to PNU-120596 (D, H, L) at 46 days of differentiation.

Figure 5. Alterations in calcium transients after treatment with pharmacological agents acting on alpha7 nAChRs.

(A-B) Representative confocal microscopy images were obtained, and calcium signals were measured in Fluo-4 loaded 62F-derived neurons, before (A) and after (B) addition of choline and PNU-120596. (scale bar = 100 μM, artificial colouring) (C) Choline alone elicits subtle changes in calcium transients; however, after the addition of PNU-120596, calcium activity increased dramatically. (D) PNU-120596 alone can evoke calcium transients in neurons that are further increased by the addition of choline. (E) MLA abolishes the effects of both PNU-120596 alone and PNU-120596+choline. (F) High-dose choline elicits an observable but transient calcium-wave. Abbreviations: cho: Choline (40 μM), CHO: Choline (4 mM), MLA:

methyllycaconitine (10 µM), PNU: PNU-120596 (4 µM), KCl: Potassium chloride, 50 mM, F/F0: Fluorescence intensity normalised to baseline activity.

Figure 6. Overall intensity changes in calcium fluorescence after addition of different alpha7 nAChR pharmacological agents and KCl.

The bar graph shows the change in maximum intensity of each cell in response to a given treatment, after 41 days of differentiation, of hiPS-62F-derived neurons calculated from 2-7 biological parallels. Each triangle represents one cell (N=130-1300). Fmax/F0 fluorescent intensities were calculated by determining average basal activity(F0) and maximal values (Fmax) after the indicated treatments. For statistical comparison between subjects, the Kruskal-Wallis test was performed.

Supplementary Files

This is a list of supplementary files associated with this preprint. Click to download.

- Vinczeetalalpha720260310PharmacologicalReportsSupplementary.docx